ChemComm

RSC Publishing

COMMUNICATION

Folic acid conjugated self-assembled layered double hydroxide nanoparticles for high-efficacy-targeted drug delivery†

Cite this: *Chem. Commun.*, 2013, **49**, 10938

Received 26th July 2013,
Accepted 2nd October 2013

DOI: 10.1039/c3cc45714a

www.rsc.org/chemcomm

Li Yan,[ab] Wei Chen,[ab] Xiaoyue Zhu,[ab] Longbiao Huang,[ab] Zhigang Wang,[c] Guangyu Zhu,[c] V. A. L. Roy,[ab] K. N. Yu[a] and Xianfeng Chen*[ab]

Enhanced selectivity and efficacy is important for advanced drug delivery. Herein, a novel type of folic acid conjugated self-assembled layered double hydroxide nanoparticles is reported. These nanoparticles have a drug loading capacity of 27 wt% and are able to enter cell nuclei and dramatically improve the efficacy of MTX.

Lack of selectivity and low efficiency of cellular internalization of anticancer agents are among the major obstacles in chemotherapy of cancer.[1,2] In recent years, many efforts have been made to increase the intracellular delivery efficacy of anticancer drugs or other biomolecules, which include viral vectors,[3] cell-penetrating peptide vectors,[4] micro/nano injections,[5] nanoneedle arrays[6] and nanoparticles. Among these approaches, the nanoparticle drug delivery system is one of the most studied. In order to increase anticancer drug selectivity and intracellular delivery efficacy, many nanoparticle drug delivery systems have been designed for cancer treatment.[7–9]

Layered double hydroxide (LDH) nanoparticles are promising nanomaterials for drug delivery because of their high drug loading capacity, low toxicity and pH-responsive drug release.[10] Drugs and biomolecules can be uploaded by co-precipitation (adding drugs during LDH preparation)[11–13] or ion-exchange (adding drugs after LDH preparation to replace the ions in the gallery between LDH layers).[10,14–17] These processes often involve high temperature. For example, for co-precipitation, drugs need to be hydrothermally treated at 100 °C.[11] For ion-exchange, the process is performed at 60 °C for 2–3 days.[14,16] Another major disadvantage of LDH nanoparticles is the difficulty in surface modification. Until recently, Choy *et al.* reported cancer-cell-specific ligand conjugated LDH nanoparticles for enhanced drug delivery.[1] During the fabrication process, an anticancer drug was loaded to LDH nanoparticles in an organic solvent at a high temperature (90 °C) for 36 hours. These harsh conditions may be detrimental to sensitive drugs and are not applicable to unstable biomolecules.

Here, we fabricated a novel type of self-assembled LDH nanoparticles. Firstly, LDH nanoparticles were prepared by a co-precipitation method in the presence of sodium dodecyl sulfate (SDS). The product is termed as LDH–SDS. SDS is used for expanding the gallery of LDH nanoparticles.[18] The X-ray diffraction (XRD) patterns (Fig. S1, ESI†) show that the (003) diffraction peak of LDH–SDS nanoparticles moves to 3.4° compared with that of pristine LDH nanoparticles (11.5°) without adding SDS during preparation. This indicates that the gallery space expanded from 7.69 to 26.0 Å. Fourier transform infrared spectra (FTIR) (Fig. S2, ESI†) show that SDS molecule peaks appear in LDH–SDS samples, which confirms the presence of SDS molecules in LDH–SDS nanoparticles.

Secondly, FA molecules were covalently attached to (3-aminopropyl) triethoxysilane (APTES) in the presence of *N*-(3-dimethylaminopropyl)-*N*-ethylcarbodiimide hydrochloride (EDC). The product is denoted as APTES-FA. Subsequently, APTES-FA was reacted with LDH–SDS nanoparticles for 24 hours in methylene chloride with *N*-cetyl-*N*,*N*,*N*-trimethylammonium (CTAB), under ultrasonication for the first 30 minutes. The final product is termed as LDH-Si-FA. CTAB is used to extract SDS molecules which are in the gallery of the LDH nanoparticles by forming hydrophobic salts between SDS and CTAB.[18] The XRD pattern in Fig. S1 (ESI†) shows the disappearance of the 3.4° peak in LDH-Si-FA, indicating the extraction of SDS molecules from LDH–SDS nanoparticles. After this step, most LDH nanoparticles lost their originally ordered layered structure, which is indicated by the remaining extremely weak peak in the XRD pattern of LDH-Si-FA. The probable mechanism is shown in Scheme S1 (ESI†). Upon strong ultrasonication, LDH–SDS nanoparticles defoliated and APTES connected many LDH layers together and assembled to form amorphous nanoparticles. The peak at 11.5° further confirms that SDS molecules were removed from LDH–SDS nanoparticles and the gallery spacing returned to the same value as that of pristine LDH nanoparticles. This is also in line with the TEM observation of a number of small unassembled LDH nanoparticles. These LDH nanoparticles still have

[a] *Department of Physics and Materials Science, City University of Hong Kong, Hong Kong SAR, China. E-mail: xianfeng.chen@cityu.edu.hk; Fax: +852-34420538; Tel: +852-34427813*

[b] *Center of Super-Diamond and Advanced Films (COSDAF), City University of Hong Kong, Hong Kong SAR, China*

[c] *Department of Biology and Chemistry, City University of Hong Kong, Hong Kong SAR, China*

† Electronic supplementary information (ESI) available: Details of experimental section, scheme of self-assembly, atomic composition, and XRD and FTIR spectra. See DOI: 10.1039/c3cc45714a

a crystal structure, indicated by the XRD peak at 11.5°. Fourier transform infrared spectra (FTIR) (Fig. S2, ESI†) show that, after reaction, the peaks of SDS molecules are significantly diminished in the LDH-Si-FA sample. Again, it reveals the extraction of SDS. Two peaks at around 1000–1200 cm^{-1} indicated by the two dots in Fig. S2 (ESI†) correspond to Si–O–Si vibration, which indicates successful attachment of APTES-FA to the LDH nanoparticles.[19,20] To further confirm this, energy-dispersive X-ray spectroscopy (EDS) analysis was performed to analyze the atomic composition of LDH-Si-FA, as shown in Table S1 (ESI†). The presence of Si (2.27 ± 0.50%, atomic percentage) indicates the successful attachment of APTES molecules to LDH nanoparticles.

The FA conjugated LDH nanoparticles were then characterized by transmission electron microscopy (TEM), and the results are shown in Fig. 1. From the TEM image, it can be seen that many LDH nanoparticles are no longer sheet-like. It appears that self-assembly happens between LDH nanoparticles. The size of these nanoparticles is about 200 nm. The nanoparticles are well distributed without aggregation and have similar size and morphology. In Fig. 1A, we can also find individual LDH nanoparticles (grey particles) with a size of about 50 nm. The appearance of individual LDH nanoparticles is consistent with our XRD data, which show a small peak at 11.5° (Fig. S1, ESI†). Upon further magnification of the FA conjugated self-assembled LDH nanoparticles (Fig. 1B), it can be observed that these nanoparticles have a porous structure. The dynamic particle size and surface charge of these FA conjugated LDH nanoparticles in aqueous solution were then measured by dynamic light scattering and the data are presented in Fig. 1C and D. The size distribution of the LDH nanoparticles is about 190 nm on average without any aggregation, which is similar to the TEM observation. The nanoparticles are positively charged (+47 mV), which makes it convenient for them to adsorb negatively charged drug molecules.

Before drug uploading, we covalently attached a fluorescein sodium salt to LDH nanoparticles to investigate their intracellular delivery using confocal fluorescent microscopy. Fluorescein sodium salt molecules were covalently conjugated to LDH nanoparticles in the same way as that used for attaching FA. It should be noted that these fluorescent nanoparticles were not attached to FA targeting molecules. Fig. 2A, B, D and E are representative confocal fluorescence microscopy images of HeLa cells after being incubated with nanoparticles for 14 hours. Fig. 2A and B show that the fluorescein sodium salt is distributed in whole cells. Attractively, in many cells, the fluorescein molecules were observed to be predominant in nuclei, as shown in Fig. 2D and E. The distribution of the fluorescein molecules in these cells can also be clearly demonstrated by the fluorescence intensity profiles shown in Fig. 2C and F.

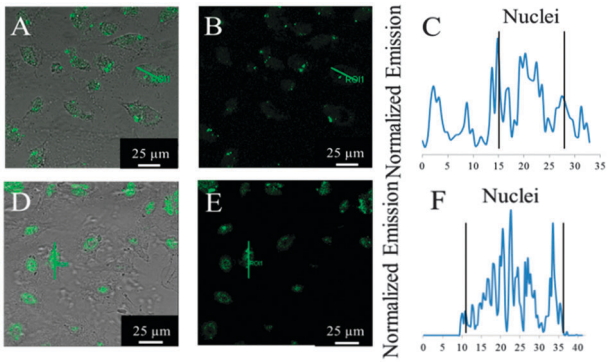

Fig. 2 Laser scanning confocal microscopy images of HeLa cells after incubation with fluorescein sodium salt conjugated LDH nanoparticles for 14 hours (A–B and D–E). (C) and (F) show the normalized emission intensity over the lines drawn crossing over cells in (A–B) and (D–E), respectively.

From the confocal microscopy results, we conclude that the self-assembled LDH nanoparticles can not only aid molecule delivery to the cytoplasm of cells, but also actively transport to the region around nuclei or even to nuclei. This will be very useful in delivering drug molecules which need to enter cell nuclei to be functional. Therefore, we hypothesize that this type of self-assembled LDH nanoparticles can significantly increase the efficacy of anticancer drugs which work by damaging the DNA of cancer cells, because they can carry anticancer drugs to cell nuclei. Here we choose the anticancer drug MTX, because it is widely used for cancer treatment, and it works by interacting with DNA to induce the apoptosis of cancer cells.[14,21–23] For drug loading, 2 mg ml^{-1} of free MTX and 2 mg ml^{-1} of FA-conjugate self-assembled LDH nanoparticles were mixed for 24 hours. By measuring the UV-Vis absorbance at 370 nm, it was found that the loading capacity of our FA-conjugated self-assembled LDH nanoparticles is 27.4 wt%.

Fig. 3 shows the viabilities of HeLa cells after being incubated with self-assembled LDH nanoparticles, free MTX and nanoparticles with MTX loading. In group 1, the NP, MTX and NP–MTX solutions contain 5 μg ml^{-1} of NP, 2 μg ml^{-1} of MTX and 5 μg ml^{-1} of NP plus 1.37 μg ml^{-1} of MTX, respectively. From groups 1 to 5, the solutions were serially diluted 3 times. After 48 hours of treatment, we observed very effective cancer cell killing in the case of MTX loaded self-assembled LDH nanoparticles, in comparison with free MTX. For example, for the HeLa cells in group 2, the viability of cells was above 60% when the cells were treated with free MTX (0.67 μg ml^{-1}).

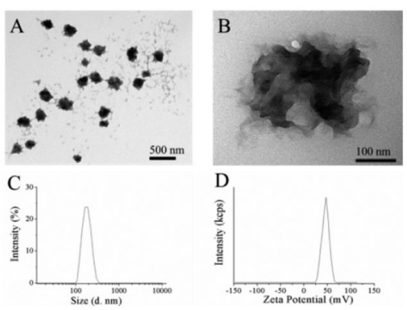

Fig. 1 (A and B) TEM images of well dispersed FA-conjugated self-assembled LDH nanoparticles. (C) Particle size distribution of the LDH nanoparticles. (D) The zeta potential of the LDH nanoparticles in aqueous and buffer-free solution.

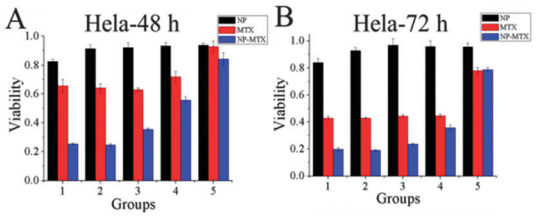

Fig. 3 The viabilities of HeLa cells after 48 (A) and 72 (B) hours of incubation with FA-conjugated LDH nanoparticles (NP), free MTX anticancer drug (MTX) and the LDH nanoparticles loaded with MTX (NP–MTX).

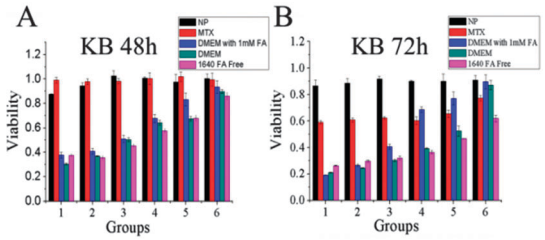

Fig. 4 The viabilities of KB cells after 48 (A) and 72 (B) hours of incubation with FA-conjugated LDH nanoparticles (NP), free MTX anticancer drug (MTX) and the nanoparticles loaded with MTX. FA-conjugated self-assembled LDH nanoparticles and free MTX were in DMEM medium. MTX loaded FA-conjugated self-assembled LDH nanoparticles were placed in three different media: (1) 1640 FA free medium; (2) DMEM medium; (3) DMEM medium with 1 mM FA.

The LDH nanoparticles did not cause significant cell death, which is indicated by the viability of cells over 90%. In great contrast, if the nanoparticles were loaded with MTX (0.46 μg ml^{-1}), the cell viability dramatically dropped to below 30%. It is worth noting that the viability of the cancer cells in group 4 which were treated with MTX loaded LDH nanoparticles (only 0.05 μg ml^{-1} MTX) was lower than that of the cells in group 1 which were incubated with free MTX drug at a concentration of 2 μg ml^{-1} ($p < 0.01$, Student *t*-test). Overall, FA-LDH nanoparticles loaded with MTX perform much better in killing cancer cells in comparison with free MTX.

After confirming that the FA-conjugated self-assembled LDH nanoparticles can greatly improve the efficacy of MTX, we investigated the targeting effect of FA ligands using KB cells which are widely considered as folate over-expressing cells. We cultured the cells with FA-conjugated self-assembled LDH nanoparticles and free MTX in DMEM medium. Then MTX loaded FA-conjugated self-assembled LDH nanoparticles were placed in three different media: (1) RPMI 1640 FA free medium (the cells in this medium are considered as high folate expressing KB cells); (2) DMEM medium (the cells in this medium are considered as low folate expressing KB cells, because it contains FA); (3) DMEM medium with 1 mM FA (the cells in this medium are considered as folate-receptor blocking KB cells). Fig. 4 shows the KB cell viabilities after treatment for 48 hours (A) and 72 hours (B).

After 48 hours of treatment, enhanced MTX efficacy was observed. For free MTX, there was almost no cell viability reduction at all concentrations (up to 2 μg ml^{-1}). In comparison, the cell viability dramatically reduced to 50% or below for groups 1 to 3 when treated with MTX loaded FA-conjugated self-assembled LDH nanoparticles (MTX concentration: 1.37 to 0.15 μg ml^{-1}). In other words, the viability of the KB cells treated with 2 μg ml^{-1} of MTX was almost 100% while that of the cells incubated with the LDH nanoparticles loaded with 0.15 μg ml^{-1} of MTX was only around 50%. This suggests a significant improvement in MTX efficacy. After 72 hours of treatment, the viabilities of the cells treated with free MTX started to drop, but MTX loaded FA-conjugated self-assembled LDH nanoparticles still performed much better. For example, the viabilities of the cells treated with free MTX in group 1 (2 μg ml^{-1}) and those treated with the nanoparticles loaded with MTX in 1640 FA free medium (0.0056 μg ml^{-1}) were very similar. This indicates around 350 times dose sparing. Moreover, KB cell viability in FA free medium is much lower than in medium containing FA (group 3–6, Fig. 4B), indicating that the FA ligand can further increase the drug delivery efficacy at lower concentrations.

From the cytotoxicity data, the following can be observed. In HeLa cells, after 48 hours of treatment, compared with free MTX, our LDH nanoparticles can reduce cell viability by around 40% even at lower MTX concentrations. In KB cells, the reduction of the viability of the cells treated with the nanoparticles loaded with MTX can be even up to around 70% (group 1 at 48 hours after treatment). In contrast, Choy *et al.* reported traditional LDH nanoparticles uploaded with MTX for cancer cell treatment.[14] In this study, the LDH nanoparticles could only reduce the cell viability by 10–20% when compared with free MTX.

In summary, we successfully fabricated a novel type of self-assembled LDH nanoparticles for high-efficacy-targeted delivery. Using confocal microscopy, it was found that fluorescein sodium salt conjugated self-assembled LDH nanoparticles showed a very strong cell membrane and nuclei penetration ability. The nanoparticles have very high drug loading efficacy (27.4 wt%). The cell viability results of HeLa and KB cells suggested that our self-assembled LDH nanoparticles have significantly enhanced MTX efficacy. We anticipate that many other targeting moieties such as proteins having free carboxyl groups can also be attached to our LDH nanoparticles by the same method.

Notes and references

1 J. Oh, S. Choi, G. Lee, S. Han and J. Choy, *Adv. Funct. Mater.*, 2009, **19**, 1617.
2 B. Rihova, *Adv. Drug Delivery Rev.*, 1998, **29**, 273.
3 M. Kay, J. Glorioso and L. Naldini, *Nat. Med.*, 2001, **7**, 33–40.
4 B. Gupta, T. Levchenko and V. Torchilin, *Adv. Drug Delivery Rev.*, 2005, **57**, 637.
5 J. Leonetti, N. Mechti, G. Degols, C. Gagnor and B. Lebleu, *Proc. Natl. Acad. Sci. U. S. A.*, 1991, **88**, 2702.
6 X. Chen, G. Zhu, Y. Yang, B. Wang, L. Yan, K. Y. Zhang, K. K. Lo and W. Zhang, *Adv. Healthcare Mater.*, 2013, **2**, 1103.
7 F. Tang, L. Li and D. Chen, *Adv. Mater.*, 2012, **24**, 1504.
8 R. A. Sperling, P. Rivera gil, F. Zhang, M. Zanella and W. J. Parak, *Chem. Soc. Rev.*, 2008, **37**, 1896.
9 K. Ariga, Q. Ji, M. J. McShane, Y. M. Lvov, A. Vinu and J. P. Hill, *Chem. Mater.*, 2012, **24**, 728.
10 K. Ladewig, M. Niebert, Z. P. Xu, P. P. Gray and G. Q. M. Lu, *Biomaterials*, 2010, **31**, 1821.
11 Z. Gu, B. E. Rolfe, A. C. Thomas, J. H. Campbell, G. Q. Lu and Z. P. Xu, *Biomaterials*, 2011, **32**, 7234.
12 S. Choi, G. E. Choi, J. Oh, Y. Oh, M. Park and J. Choy, *J. Mater. Chem.*, 2010, **20**, 9463.
13 Z. Gu, A. C. Thomas, Z. P. Xu, J. H. Campbell and G. Q. Lu, *Chem. Mater.*, 2008, **20**, 3715.
14 J. Choy, J. Jung, J. Oh, M. Park, J. Jeong, Y. Kang and O. Han, *Biomaterials*, 2004, **25**, 3059.
15 Y. Wong, K. Markham, Z. P. Xu, M. Chen, G. Q. Max Lu, P. F. Bartlett and H. M. Cooper, *Biomaterials*, 2010, **31**, 8770.
16 J. Choy, S. Kwak, Y. Jeong and J. Park, *Angew. Chem., Int. Ed.*, 2000, **39**, 4042.
17 A. Li, L. Qin, W. Wang, R. Zhu, Y. Yu, H. Liu and S. Wang, *Biomaterials*, 2011, **32**, 469.
18 A. Park, H. Kwon, A. Woo and S. Kim, *Adv. Mater.*, 2005, **17**, 106.
19 Y. Wang, Y. Wang, P. Cao, Y. Li and H. Li, *CrystEngComm*, 2011, **13**, 177.
20 M. Karakassides, D. Petridis and D. Gournis, *Clays Clay Miner.*, 1997, **45**, 649.
21 J. McGuire, *Curr. Pharm. Des.*, 2003, **9**, 2593.
22 J. Yuan, W. Guo, X. Yang and E. Wang, *Anal. Chem.*, 2009, **81**, 362.
23 W. Huang, P. Yang, Y. Chang, V. E. Marquez and C. Chen, *Biochem. Pharmacol.*, 2011, **81**, 510.

